Thermal Conduction Normal to Thin Silicon Nitride Films on Diamond and GaN

Jungwan Cho[1], Kenneth K. Chu [2], Pane C. Chao[2], Craig McGray[3], Mehdi Asheghi[1], and Kenneth E. Goodson[1]
[1)] Department of Mechanical Engineering, Stanford University, Stanford, CA, 94305, USA
[2)] Microelectronics Center, BAE Systems, Nashua, NH, 03060, USA
[3)] Modern Microsystems, Inc., Silver Spring, MD, 20902, USA
Email: jungwan.cho@stanford.edu

ABSTRACT

Self-heating effects severely limit the performance of high-power gallium nitride (GaN) high-electron-mobility transistors (HEMTs). High thermal resistances within micrometers of the transistor junction often dominate the junction temperature rise and fundamentally restrict the device power handling capability. The use of high-thermal-conductivity diamond near the junction can address this thermal limitation, but this approach requires careful attention to the quality of the thermal interface between the GaN and diamond. Here we use time-domain thermoreflectance (TDTR) to measure thermal resistances of thin silicon nitride (SiN) films with varying thicknesses on both diamond and GaN. Measurement of these two sets of samples provides an estimate for the thermal resistance between the GaN and diamond since the SiN film can be used as a bonding layer between the two materials. The effective resistances of the SiN film and bottom interface (SiN/diamond or SiN/GaN) range from 22 to 37 m^2 K GW^{-1} for both sets of samples. Our findings suggest the possibility of achieving 22 m^2 K GW^{-1} as the GaN/diamond thermal interface resistance.

KEY WORDS: High-Electron-Mobility Transistors (HEMT), Gallium Nitride (GaN), Silicon Nitride (SiN), Diamond, Thermal Boundary Resistance (TBR), Thermal Conductivity, Time-Domain Thermoreflectance (TDTR)

NOMENCLATURE

d	thickness (nm)
k	thermal conductivity (W m^{-1} K^{-1})
R	thermal resistance (10^{-9} m^2 K W^{-1})
V	voltage signal (V)

Subscripts

Al	aluminum
b	boundary
diam	diamond
eff	effective
GaN	gallium nitride
in	in-phase
out	out-of-phase
SiN	silicon nitride
T	total

I. INTRODUCTION

High-electron-mobility transistors (HEMTs) based on gallium nitride (GaN) are promising for a wide variety of high power electronic applications due to their superior high-power and high-frequency performance [1]–[3]. Much progress has been made over the past decade in increasing the maximum power density from around 10 W/mm [1] to more than 40 W/mm [2] for GaN HEMT on SiC. However, due to junction self-heating and associated thermal constraints, GaN HEMT devices on SiC are typically operated at a much lower power level [4], [5]. High thermal resistances within micrometers of the transistor junction (i.e., in the "near-junction" region) often impede efficient heat dissipation from active device regions [4], [6], [7]. Integration of chemical-vapor-deposited (CVD) diamond in the near-junction region can address this thermal limitation owing to its superior heat spreading capability compared to that of SiC. Composite GaN substrates containing CVD diamond can offer local thermal conductivities higher by a factor of nearly 5 than SiC [7]. However the fabrication of GaN on diamond substrates is very challenging due to the much larger lattice and coefficient of thermal expansion (CTE) mismatches between GaN and diamond than those between GaN and SiC [8], [9].

Prior works have demonstrated the direct growth of AlGaN/GaN heterostructures on single-crystal diamond with relatively thick transition layers (approximately 1 µm) [9]–[11]. Since such thick transition layers often exhibit low thermal conductivity [12], this approach can result in high thermal resistance between the GaN and diamond. An alternative approach involves epitaxial transfer of AlGaN/GaN heterostructures to CVD diamond using a bonding layer thinner than 50 nm [5], [12]–[14]. This approach often uses a high-temperature (> 800 °C) GaN/diamond bonding process [13], but a low-temperature (room temperature) bonding technology has recently been demonstrated to minimize the impact of CTE mismatch between GaN and diamond [15]. Despite all these efforts, the current GaN on diamond technologies still can result in high concentrations of defects or fully amorphous regions near the GaN-diamond interface. More progress must still be made to minimize the thermal resistance at the GaN/diamond interface and identify the specific microstructural causes for the resistance.

This work investigates the through-plane thermal conduction in thin silicon nitride (SiN) films with varying thicknesses on both GaN and diamond using time-domain

thermoreflectance (TDTR). With these two sets of samples we provide an estimate for the GaN/diamond thermal interface resistance since the SiN film can serve as a bonding layer between the GaN and diamond. The two sets of samples consist of SiN films with thicknesses of 13, 24, and 36 nm on diamond and of 12, 23, and 35 nm on GaN. For each set of samples, we extract the effective thermal resistance, which combines the volumetric SiN resistance and the boundary resistance at the SiN interface with the underlying material (diamond or GaN). The data suggest that the GaN/diamond thermal interface resistance can be close to 22 m^2 K GW^{-1} using 23-24 nm SiN film.

II. SAMPLES AND EXPERIMENTAL METHODS

Figure 1 illustrates cross-sectional schematic drawings of two configurations of the SiN samples used in this study: one is the SiN on diamond and the other is the SiN on GaN. Three SiN films with thicknesses of 13, 24, and 36 nm were grown on a diamond substrate by plasma-enhanced chemical vapor deposition (PECVD) at 300 ℃. The diamond substrate was polished and chemically cleaned before the SiN film deposition. Similarly, three SiN films with thicknesses of 12, 23, and 35 nm were grown on a 1.8-µm-thick GaN on a SiC substrate. Approximately 53 nm of Al was deposited by e-beam evaporation on all the samples studied here after an extended air break; the Al serves as the transducer for thermoreflectance measurements.

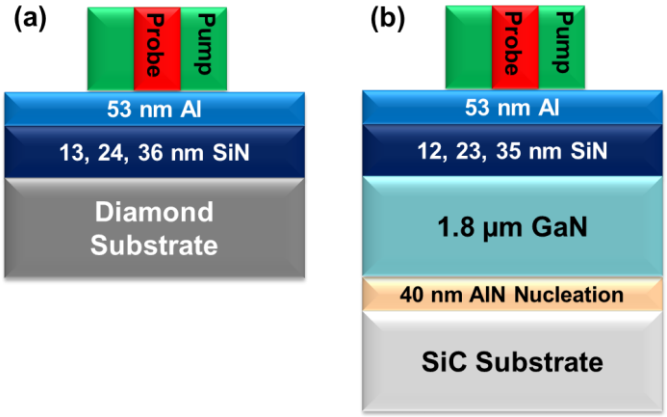

Fig. 1: Cross-sectional schematic drawings of SiN samples on (a) a diamond substrate and (b) on a 1.8 µm GaN on SiC. For the latter case, a 40 nm AlN nucleation layer is placed between the GaN and SiC to minimize lattice mismatch stress. For both configurations of the SiN samples, evaporated Al layers of 53 nm serve as the metal transducers for thermoreflectance measurements. The green and red areas indicate the pump and probe beams, respectively.

Thermal conduction normal to the SiN films on diamond and GaN is investigated by TDTR [16]–[21]. TDTR is an optical pump-probe technique that measures the temperature response of a sample surface to modulated laser heating. In our setup, a mode-locked Nd:YVO4 laser generates 9.2 ps optical pulses at 1064 nm wavelength and with 82 MHz repetition rate, which are split into a pump and probe component. The pump beam is modulated at 2 MHz and 8 MHz by an electro-optic modulator (EOM) for lock-in detection, and then frequency-doubled to 532 nm by a second harmonic generation (SHG) for the spectral separation of the pump and the probe. The pump beam is then directed onto the sample through a microscope objective lens and deposits heat in the metal transducer (Al in our samples). The probe beam is temporally delayed relative to the pump optical heating by a mechanical delay stage and then passes through a single-mode fiber (SMF) to minimize errors associated with beam divergence and beam overlap due to the delay stage motion. The probe beam is then directed onto the sample through the same microscope objective (coaxial with the pump beam). The reflected probe beam from the sample surface is collimated through the objective and then directed to a photodetector connected to an RF lock-in amplifier. The lock-in amplifier detects the temperature-induced changes in intensity of the reflected probe beam at the pump modulation frequency and as a function of the pump-probe delay time, i.e., it measures the temporal response of the surface temperature of the metal transducer film via the thermoreflectance. Further details of our TDTR setup are described in [20] and [21].

We monitor the amplitude $\sqrt{V_{in}^2 + V_{out}^2}$ of the in-phase $V_{in}(t)$ and out-of-phase $V_{out}(t)$ components of the thermoreflectance signal detected by the lock-in amplifier over 3.5 ns of probe delay time t. The amplitude signal is compared to the solution of the three-dimensional radial-symmetric heat diffusion equation for the multilayer stack with modulated optical surface heating to extract the thermal properties of the films and interfaces underneath the metal transducer [17]. We use bulk values for the heat capacity and thermal conductivity of the Al film [22], [23]. The heat capacities of the other constituent layers are taken from the literature [24]–[26]. The thermal conductivity of the GaN film is measured separately using TDTR, yielding k_{GaN} = 170 ± 10 W m^{-1} K^{-1}. We use 1500 W m^{-1} K^{-1} as the thermal conductivity of the diamond substrate, which is taken from manufacturer specification. This procedure leaves three unknowns in the multi-layer thermal model: a) the thermal boundary resistance (TBR) at the Al-SiN interface $R_{b,Al-SiN}$, b) the through-plane thermal conductivity of the SiN k_{SiN}, and c) the TBR at the SiN-diamond (or SiN-GaN) interface $R_{b,SiN-diam}$ (or $R_{b,SiN-GaN}$).

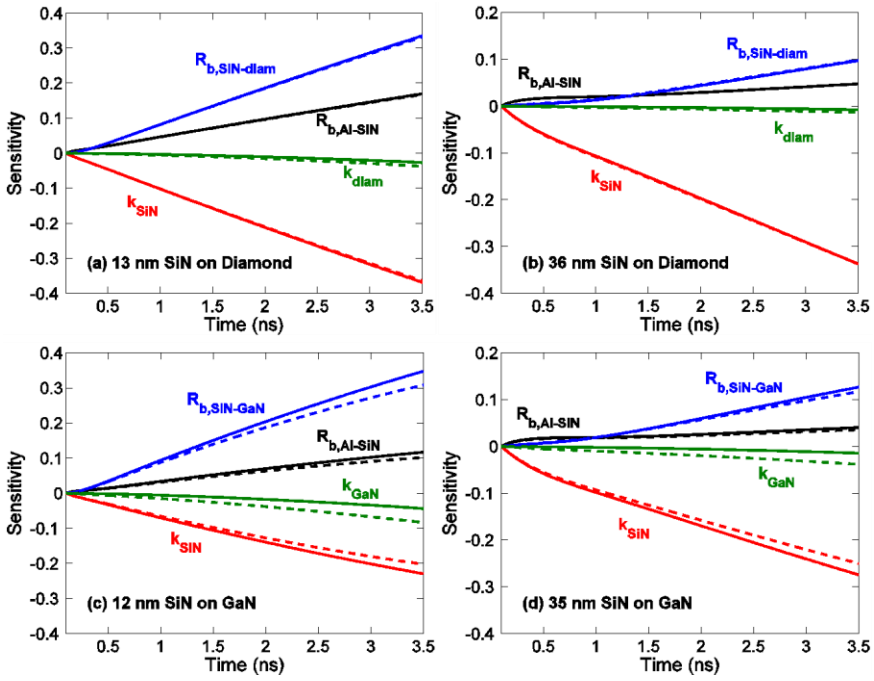

Fig. 2: Sensitivity S_{α} to changes in four parameters in the multi-layer thermal model as a function of delay time for the (a) 13 nm SiN and (b) 36 nm SiN on diamond, and the (c) 12 nm SiN and (d) 35 nm SiN on GaN—all at room temperature—calculated by Eq. (1). Sensitivity values are evaluated at a pump modulation frequency of 2 MHz (dashed lines) and 8 MHz (solid lines). Black lines represent the sensitivity to the Al/SiN thermal boundary resistance (TBR) $R_{b,Al-SiN}$, red lines represent the sensitivity to the SiN thermal conductivity k_{SiN}, blue lines represent the sensitivity to the SiN/diamond TBR $R_{b,SiN-diam}$ (or to the SiN/GaN TBR $R_{b,SiN-GaN}$), and green lines represent the sensitivity to the diamond thermal conductivity k_{diam} (or to the GaN thermal conductivity k_{GaN}).

III. SENSIVIVITY ANALYSIS

We study the sensitivity of the measurement to the three unknown parameters— $R_{b,Al-SiN}$, k_{SiN}, and $R_{b,SiN-diam}$ (or $R_{b,SiN-GaN}$)—and the thermal conductivities of the diamond substrate and the GaN film (k_{diam} and k_{GaN}). The sensitivity of the amplitude data to these parameters (which are denoted by α here) is defined as the logarithmic derivative of the amplitude data $\sqrt{V_{in}{}^2 + V_{out}{}^2}$ with respect to α [21],

$$S_{\alpha} = \frac{\partial \ln(\sqrt{V_{in}{}^2 + V_{out}{}^2})}{\partial \ln \alpha}. \qquad (1)$$

Figure 2 shows the sensitivity of the amplitude to $R_{b,Al-SiN}$, k_{SiN}, $R_{b,SiN-diam}$ (or $R_{b,SiN-GaN}$), and k_{diam} (or k_{GaN}) for the thinnest and thickest SiN samples in both configurations at room temperature. The sensitivity values are plotted as a function of the probe delay time and at the pump modulation frequencies of 2 MHz and 8 MHz. Best-fit values are assumed for the three unknown parameters of each sample.

For the thinnest SiN samples of both configurations (see Figs. 2(a) and 2(c)), the sensitivities to $R_{b,Al-SiN}$, k_{SiN}, and $R_{b,SiN-diam}$ (or $R_{b,SiN-GaN}$) are similar in shape over the entire range of delay time and their absolute values are comparable. Thus, the measurement for the thinnest sample is only sensitive to the total summed resistance R_T:

$$R_T = R_{b,\mathrm{Al}-SiN} + R_{SiN}\left(=\frac{d_{SiN}}{k_{SiN}}\right) + R_{b,SiN-diam}\,(\text{or } R_{b,SiN-GaN}), \qquad (2)$$

where R_{SiN} is the SiN intrinsic resistance and d_{SiN} is the SiN film thickness. For the other four, thicker, samples, the sensitivity to $R_{b,Al-SiN}$ is different in curvature from those to k_{SiN} and $R_{b,SiN-diam}$ (or $R_{b,SiN-GaN}$), and its absolute values are lower than those of the other two components. This allows us to isolate the Al/SiN TBR from the SiN intrinsic resistance and the SiN/diamond (or SiN/GaN) TBR. The latter two components are combined into an effective SiN resistance $R_{SiN,\,eff}$, which can be expressed as

$$R_{SiN,eff} = R_{SiN}(=\frac{d_{SiN}}{k_{SiN}}) + R_{b,SiN-diam}(\text{or } R_{b,SiN-GaN}). \quad (3)$$

The sensitivity to the diamond thermal conductivity is almost negligible over most of the delay time (see Figs. 2(a) and 2(b)) [27], whereas the sensitivity to the GaN thermal conductivity is not negligible especially for the thinnest SiN on GaN sample (see Fig. 2(c)).

IV. RESULTS AND DISCUSSION

Table I summarizes the thermal properties of each SiN sample obtained using TDTR. As discussed in Section III, we extract the total summed resistance R_T for the thinnest SiN on diamond and GaN and the effective resistance of the SiN film and bottom interface $R_{SiN,\,eff}$ for the other four samples. At room temperature, we find the total summed resistance R_T to be 17.5 ± 0.6 m^2 K GW^{-1} for the thinnest SiN on diamond sample and 17.2 ± 0.7 m^2 K GW^{-1} for the thinnest SiN on GaN sample. The effective SiN thermal resistances $R_{SiN,\,eff}$ are 21.6 ± 0.7 m^2 K GW^{-1} and 36.8 ± 0.8 m^2 K GW^{-1} for 24 nm and 36 nm SiN films on diamond, respectively. For 23 nm and 35 nm SiN films on GaN, the measured values of $R_{SiN,\,eff}$ are 22.0 ± 0.9 m^2 K GW^{-1} and 37.3 ± 1.5 m^2 K GW^{-1}, respectively. The Al-SiN TBRs range between 5 and 8 m^2 K GW^{-1} for these four samples. Uncertainty in the thickness of the Al transducer (d_{Al} = 53 ± 2 nm) determines the error bars for all measured samples.

TABLE I. Extracted thermal properties of SiN on diamond and GaN samples measured at room temperature using TDTR. $R_{b,Al-SiN}$ represents the Al-SiN TBR, $R_{SiN,\,eff}$ represents the effective SiN resistance (see Eq. (3)), and R_T represents the total summed resistance of $R_{b,Al-SiN}$ and $R_{SiN,\,eff}$ (see Eq. (2)).

Sample	$R_{b,Al-SiN}$ [m^2 K GW^{-1}]	$R_{SiN,\,eff}$ [m^2 K GW^{-1}]	R_T [m^2 K GW^{-1}]
13 nm SiN on diamond	N/A	N/A	17.5 ± 0.6
24 nm SiN on diamond	4.8 ± 0.2	21.6 ± 0.7	26.4 ± 0.9
36 nm SiN on diamond	5.5 ± 0.3	36.8 ± 0.8	42.3 ± 1.1
12 nm SiN on GaN	N/A	N/A	17.2 ± 0.7
23 nm SiN on GaN	7.5 ± 0.2	22.0 ± 0.9	29.5 ± 1.1
35 nm SiN on GaN	5.3 ± 0.3	37.3 ± 1.5	42.6 ± 1.8

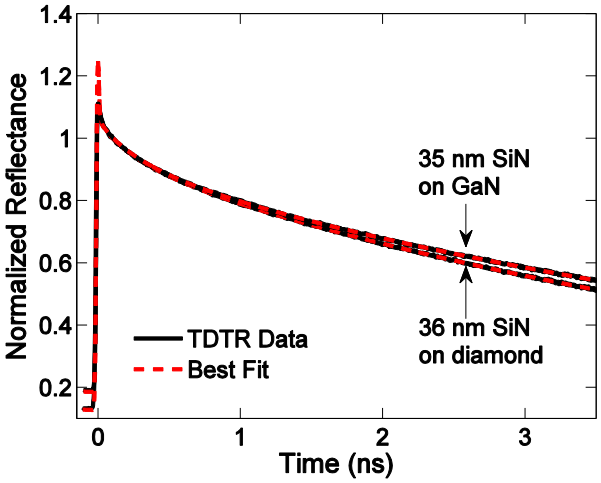

Fig. 3: (a) Representative TDTR data (black solid lines) with best analytical fits (red dashed line) for the thickest SiN films on diamond and GaN.

If we convert the effective thermal resistance of the SiN film into its effective thermal conductivity (i.e., $k_{SiN,eff} = d_{SiN} / R_{SiN,eff}$), then we obtain 1.1 W m^{-1} K^{-1} for the 24 nm SiN film on diamond and 0.98 W m^{-1} K^{-1} for the 36 nm SiN film on diamond. For 23 nm and 35 nm SiN films on GaN, these values are 1.0 W m^{-1} K^{-1} and 0.94 W m^{-1} K^{-1}, respectively.

The prior literature, including data from us, suggests that the thermal conductivities of SiN thin films can range from below 1 W/mK up to as much as 12 W/mK [24], [28], [29]. Zhang and Grigoropoulosa [28] used steady-state Joule heating and electrical-resistance thermometry to measure the thermal conductivities of two free-standing SiN films with thicknesses of 0.6 μm and 1.4 μm, both of which were prepared by low pressure chemical vapor deposition (LPCVD) at 835 °C. Near room temperature, they reported approximately 12 W m^{-1} K^{-1} and 8 W m^{-1} K^{-1} for the thermal conductivities of 0.6-μm-thick and 1.4-μm-thick SiN films, respectively. They attributed the lower thermal conductivity of their thicker film to a high presence of small voids in this film. Bai *et al.* [29] performed nanosecond transient thermoreflectance measurements to measure the thermal conductivities of LPCVD SiN films with thicknesses ranging from 37 to 200 nm grown on Si substrates at 800 °C. Their measured SiN thermal conductivities range from 1.2 to 2.1 W m^{-1} K^{-1} at room temperature and include the TBR at the SiN-Si interface. Lee and Cahill [24] measured the thermal conductivities of 21-nm-thick to 252-nm-thick SiN films, all of which were grown on Si substrates by PECVD at 300 °C, using the three-omega method. Their measured room temperature values range between 0.4 and 0.7 W m^{-1} K^{-1} and include the contributions from the two interfaces on either side of the SiN film. The very substantial variation in the prior literature is owed to the varying fractions of poly/nanocrystalline materials and density [24], [28]. Data for

other amorphous films show that annealing can improve the thermal conductivity [30].

IV. CONCLUSIONS

This work extracts the effective thermal resistances of SiN films on both diamond and GaN using TDTR. The effective SiN resistance ranges from 22 to 37 m^2 K GW^{-1} for both configurations of the samples. A recent simulation work [7] has shown that GaN-on-diamond devices with an interface resistance of below 30 m^2 K GW^{-1} can outperform GaN-on-SiC devices even with zero interface resistance in terms of the temperature rise of the device channel. Our data suggest that the GaN/diamond interface resistance can approach 22 m^2 K GW^{-1} using 23-24 nm SiN films, which is below the target interface resistance of 30 m^2 K GW^{-1}. With a further reduction in the resistance down to the lower limit (~3 m^2 K GW^{-1} [7]) predicted by the diffuse mismatch theory, GaN-on-diamond technologies will significantly improve the near-junction thermal management of GaN HEMT.

ACKNOWLEDGMENTS

The authors acknowledge financial support from BAE Systems (agreement # 842636-2, titled: Near Junction Thermal Transport), the AFOSR (agreement # FA9550-12-1-0195, titled: MultiCarrier and Low-Dimensional Thermal Conduction at Interfaces for High Power Electronic Devices), and the DARPA Microsystems Technology Office (MTO) through Air Force contract (agreement # FA8650-10-1-7044, titled: Device-Level Thermal Management for HEMT Radar: Thermal Metrology, Interfaces, and Metrics). The work of J. Cho was supported in part by a Samsung Scholarship.

REFERENCES

[1] U. K. Mishra, P. Parikh, and Y. F. Wu, "AlGaN/GaN HEMTs-An Overview of Device Operation and Applications," Proceedings of the IEEE, vol. 90, no. 6, pp. 1022–1031, Jun. 2002.

[2] Y. F. Wu, M. Moore, A. Saxler, T. Wisleder, and P. Parikh, "40-W/mm double field-plated GaN HEMTs," Proc. IEEE DRC Conf. Dig., p.151 , 2006.

[3] Y. Yue, Z. Hu, J. Guo, B. Sensale-Rodriguez, G. Li, R. Want, F. Faria, T. Fang, B. Song, X. Gao, S. Guo, T. Kosel, G. Snider, P. Fay, D. Jena, and H. Xing, "InAlN/AlN/GaN HEMTs with regrown ohmic contacts and f_T of 370 GHz," IEEE Electron Device Lett., vol. 33, no. 7, pp. 988–990, Jul. 2012.

[4] A. Bar-Cohen, J. D. Albrecht, and J. J. Maurer, "Near-Junction Thermal Management for Wide Bandgap Devices," in IEEE Symposium on Compound Semiconductor Integrated Circuit, Waikoloa, HI, Oct. 2011, pp. 1–5.

[5] D. C. Dumka, T. M. Chou, F. Faili, D. Francis, and F. Ejeckam, "AlGaN/GaN HEMTs on Diamond Substrate with over 7 W/mm Output Power Density at 10 GHz," Electronics Letters, vol. 49, no. 20, pp. 1298–1299, Sep. 2013.

[6] Y. Won, J. Cho, D. Agonafer, M. Asheghi, and K. E. Goodson, "Cooling Limits for GaN HEMT Technology," in IEEE Symposium on Compound Semiconductor Integrated Circuit, Monterey, CA, Oct. 2013, pp. 1–5.

[7] J. Cho, Z. Li, M. Asheghi, and K. E. Goodson, "Near-Junction Thermal Management: Thermal Conduction in Gallium Nitride Composite Substrates," Annu. Rev. Heat Transfer, vol. 18, 2014.

[8] E. Cho, "GaN Based Heterostructure Growth and Application to Electronic Devices and Gas Sensors," Ph.D. dissertation, Dept. Elect. Eng., Univ. of Michigan, Ann Arbor, MI, 2009.

[9] G. W. G. van Dreumel, P. T. Tinnemans, A. A. J. van den Heuvel, T. Bohnen, J. G. Buijnsters, J. J. ter Meulen, W. J. P. van Enckevort, P. R. Hageman, and E. Vlieg, "Realising epitaxial growth of GaN on (001) diamond", J. Appl. Phys., vol. 110, no. 1, 013503, July 2011.

[10] M. Alomari, A. Dussaigne, D. Martin, N. Grandjean, C. Gaquière, and E. Kohn, "AlGaN/GaN HEMT on (111) single crystalline diamond," Electron. Lett., vol. 46, no. 4, pp. 299–301, Feb. 2010.

[11] K. Hirama, M. Kasu, and Y. Taniyasu, "RF High-Power Operation of AlGaN/GaN HEMTs Epitaxially Grown on Diamond," Electron Device Letters, IEEE, vol. 33, no. 4, pp. 513–515, 2012.

[12] J. Cho, Z. Li, E. Bozorg-Grayeli, T. Kodama, D. Francis, F. Ejeckam, F. Faili, M. Asheghi, and K. E. Goodson, "Improved Thermal Interfaces of GaN-Diamond Composite Substrates for HEMT Applications," IEEE Trans. on Components, Packaging and Manufacting Technology, vol. 3, no. 1, pp. 79–85, Jan. 2013.

[13] D. Francis, F. Faili, D. Babić, F. Ejeckam, A. Nurmikko, and H. Maris, "Formation and characterization of 4-inch GaN-on-diamond substrates," Diamond and Related Materials, vol. 19, no. 2, pp. 229–233, Feb. 2010.

[14] K. D. Chabak, J. K. Gillespie, V. Miller, A. Crespo, J. Roussos, M. Trejo, D. E. Walker, Jr., G. D. Via, G. H. Jessen, J. Wasserbauer, F. Faili, D. I. Babic, D. Francis, and F. Ejeckam, "Full-Wafer Characterization of AlGaN/GaN HEMTs on Free-Standing CVD Diamond Substrates," IEEE Electron Device Lett., vol. 31, no. 2, pp. 99–101, Feb. 2010.

[15] K. K. Chu, T. Yurovchak, P. C. Chao, and C. T. Creamer, "Thermal Modeling of High Power GaN-on-Diamond HEMTs Fabricated by Low-Temperature Device Transfer Process," in IEEE Symposium on Compound Semiconductor Integrated Circuit, Monterey, CA, Oct. 2013, pp. 1–5.

[16] W. S. Capinski and H. J. Maris, "Improved apparatus for picosecond pump-and-probe optical measurements," Rev. Sci. Instrum., vol. 67, no. 8, pp. 2720–2726, Aug. 1996.

[17] D. G. Cahill, “Analysis of heat flow in layered structures for time-domain thermoreflectance,” Rev. Sci. Instrum., vol. 75, no. 12, pp. 5119–5122, Nov. 2004.
[18] A. Schmidt, M. Chiesa, X. Chen, and G. Chen, “An optical pump-probe technique for measuring the thermal conductivity of liquids,” Rev. Sci. Instrum., vol. 79, no. 6, pp. 064 902-1–064 902-5, Jun. 2008.
[19] Y. K. Koh, S. L. Singer, W. Kim, J. Zide, H. Lu, D. G. Cahill, A. Majumdar, and A. Gossard, “Comparison of the 3ω method and time-domain thermoreflectance for measurements of the cross-plane thermal conductivity of epitaxial semiconductors,” J. Appl. Phys., vol. 105, no. 5, pp. 054303-1–054303-7, Mar. 2009.
[20] M. A. Panzer, “Thermal Characterization and Modeling of Nanostructured Materials,” Ph.D. dissertation, Dept. Mech. Eng., Stanford Univ., Stanford, CA, 2010.
[21] J. Cho, Y. Li, W. E. Hoke, D. H. Altman, M. Asheghi, and K. E. Goodson, "Phonon scattering in strained transition layers for GaN heteroepitaxy,” Phys. Rev. B, Condens. Matter, vol. 89, no. 11, pp. 115301-1-115301-11, Mar. 2014.
[22] W. F. Giauque and P. F. Meads, “The Heat Capacities and Entropies of Aluminum and Copper from 15 to 300°K,” J. Am. Chem. Soc., vol. 63, no. 7, pp. 1897–1901, July 1941.
[23] C. Wei, X. Zheng, D. G. Cahill, and J.-C. Zhao, “Invited Article: Micron resolution spatially resolved measurement of heat capacity using dual-frequency time-domain thermoreflectance,” Rev. Sci. Instrum., vol. 84, no. 7, pp. 071301-1–071301-9, July 2013.
[24] S. M. Lee and D. G. Cahill, “Heat transport in thin dielectric films,” J. Appl. Phys., vol. 81, no. 6, pp. 2590–2595, Mar. 1997.
[25] I. Zięborak-Tomaszkiewicz, E. Utzig, and P. Gierycz, “Heat capacity of crystalline GaN,” J. Thermal Anal. Calorimetry, vol. 91, no. 1, pp. 329–332, 2008.
[26] J. E. Graebner, “Measurements of specific heat and mass density in CVD diamond,” Diam. Rel. Mater., vol. 5, no. 11, pp. 1366–1370, Nov. 1996.
[27] J. Cho, P. C. Chao, M. Asheghi, and K. E. Goodson, “Phonon Conduction Normal to Polysilicon Films on Diamond,” in ASME 2014 Fourth International Conference on Micro/Nanoscale Heat and Mass Transfer, Hong Kong, China, 2013.
[28] X. Zhang and C. P. Grigoropoulos, “Thermal conductivity and diffusivity of free-standing silicon nitride thin films,” Rev. Sci. Instrum., vol. 66, no. 2, pp. 1115–1120, Feb. 1995.
[29] S. Bai, Z. Tang, Z. Huang, and J. Yu, "Thermal characterization of Si_3N_4 thin films using transient thermoreflectance technique," IEEE Trans. Ind. Electron., vol. 56, no. 8, pp.3238–3243, Aug. 2009.
[30] K. E. Goodson, M. I. Flik, L. T. Su, and D. A. Antoniadis, “Annealing-temperature dependence of the thermal conductivity of LPCVD silicon-dioxide layers,” IEEE Electron Device Lett., vol. 14, no. 10, pp. 490–492, Oct. 1993.